

Synthesis and inhibition corrosion effect of two thiazole derivatives for carbon steel in 1 M HCl

O. Benali^{1*}, M. Zebida^{1,2}, U. Maschke³

¹*Laboratory of Chemistry: Synthesis, Properties and Applications, University of Saida – Dr.
Moulay Tahar, Algeria.*

²*Department of Chemistry, Faculty of sciences, University of Saida – Dr. Moulay Tahar,
Algeria.*

³*Unité Matériaux et Transformations: Ingénierie des systèmes polymères (UMIST :ISP),
Université Lille1, France*

**Corresponding author: benaliomar@hotmail.com*

Abstract

Inhibition of C38 carbon steel corrosion by 4-methyl-3-phenyl-2(3H)-thiazolethione (**TO1**) and 4-methyl-2-(methylthio)-3- phenylthiazol-3-ium (**ST1**) in 1 M HCl was investigated by weight loss and electrochemical methods. All of the data obtained reveal that the two compounds act as good inhibitors in this media. At optimized concentration **TO1** and **ST1** showed the highest inhibition efficiency of 98.8 % (2.10^{-4} M) and 93.86 % (10^{-3} M) respectively. Polarization curves show that inhibitor molecules act as mixed type inhibitors. The impedance study showed that an increase in the concentration of the two inhibitors is accompanied by an increase in polarization resistance and a decrease in double layer capacitance. The Langmuir isotherm very well describes the adsorption of inhibitors to the surface of the corroding metal and the thermodynamic parameters showed that the adsorption of the two compounds was strong and chemical nature. X-ray photoelectron spectroscopy (XPS) confirms and describes the absorption of inhibitors under investigation on the metal surface.

Keywords: Corrosion inhibition; C38 carbon steel; HCl; thiazole derivatives, XPS

1. Introduction

Carbon steel is one of the most widely used metals in the automotive industry, machinery, construction structures, among many other uses. This material has been extensively studied as a model for corrosion inhibition. This is due to the fact that carbon steel corrodes very easily in different environments, but if we talk about an acidic medium which is very corrosive, the corrosion of carbon steel increases considerably [1-4]. In general, the inhibitors are organic compounds in whose structures are oxygen, sulfur, nitrogen and phosphorous atoms and unsaturated bonds together with aromatic rings. Thiazole-type compounds have been proven to be potent corrosion inhibitors. This is due to their strong adsorption susceptibility to metal surfaces in aggressive media via their polar groups and their potential for complexing with the metal surface. In addition, they exhibit different agricultural, industrial and biological properties such as anticancer, antiviral, antibacterial, antifungal, etc. [5-18].

All of these properties have manifested their anti-toxic character. They also possess abundant lone-pair electrons and unshared electron pairs on the nitrogen atom, which can interact with any metal's d-orbitals to provide a protective film [13-14]. Thus in recent years research on derivative thiazole inhibitors has been a major topic. Researchers have made many efforts to examine new thiazole derivatives in the hope of improving its inhibition effectiveness. A common route for enhancing a given heterocycle's corrosion inhibition efficiency is to alter its structure with different moieties or functional groups [15-18].

This work is focused at synthesizing two thiazolic derivatives : 4-methyl-3-phenyl-2(3H)-thiazolethione (**TO1**) and 4-methyl-2-(methylthio)-3- phenylthiazol-3-ium (**ST1**) and study their inhibition efficiency as inhibitors for C38 carbon steel in 1M HCl solution, using electrochemical methods, weight loss measurement and XPS surface study.

2. Experimental Section

2.1 Materials

2.1.1. Composition of C38 Sample.

The pieces of steel sheet (used as working electrode and for weight loss experiments) were prepared from C38 carbon steel, where the composition and method of preparation was given in our already published work [14].

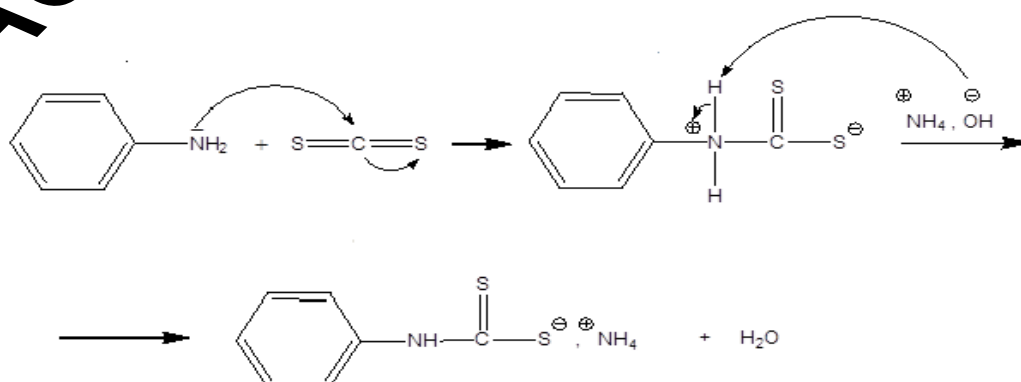
2.1.2. Solutions.

The concentration of the used inhibitors ranged from 10^{-6} M to 10^{-3} M in 1 M HCl (prepared from 37% HCl in distilled water).

2.1.3. Synthesis of corrosion inhibitors

a) 4-methyl-3-phenyl-2(3H)-thiazolethione (**TO1**)

Aniline (18.5 mL, 0.2 mol) was added dropwise on a mixture of CS_2 (14.5 mL, 0.2 mol) and 24 mL of NH_4OH , stirred at 0°C . After stirring for 2 hour at room temperature, the mixture was filtered and washed with Et_2O (3 x 25 mL) to give the yellow dithiocarbamate (30 g, 80%). 1-Chloro-2-propanone (9 mL, 0.1mol, 1 eq) was added to a suspension of (18.6 g, 0.1mol) of the dithiocarbamate salt in ethanol (20 mL). After stirring for 2 hours at r.t., 0.5 mL of HCl (36%) were added and the mixture was refluxed for 3 hour. After filtration, the solid was washed with water (3 x 5 mL) and dried to give (**TO1**) (15.13 g, 73%, mp = 146°C). Detailed reaction mechanism is presented in figure 1a and NMR spectra of **TO1** is presented in figure 1b.



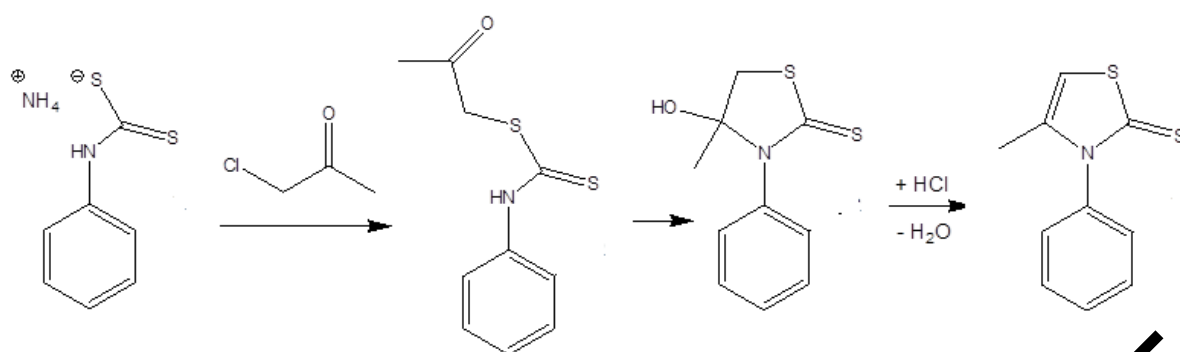


Figure 1a. Synthesis of 4-methyl-3-phenyl-2(3H)-thiazolethione (**TO1**)

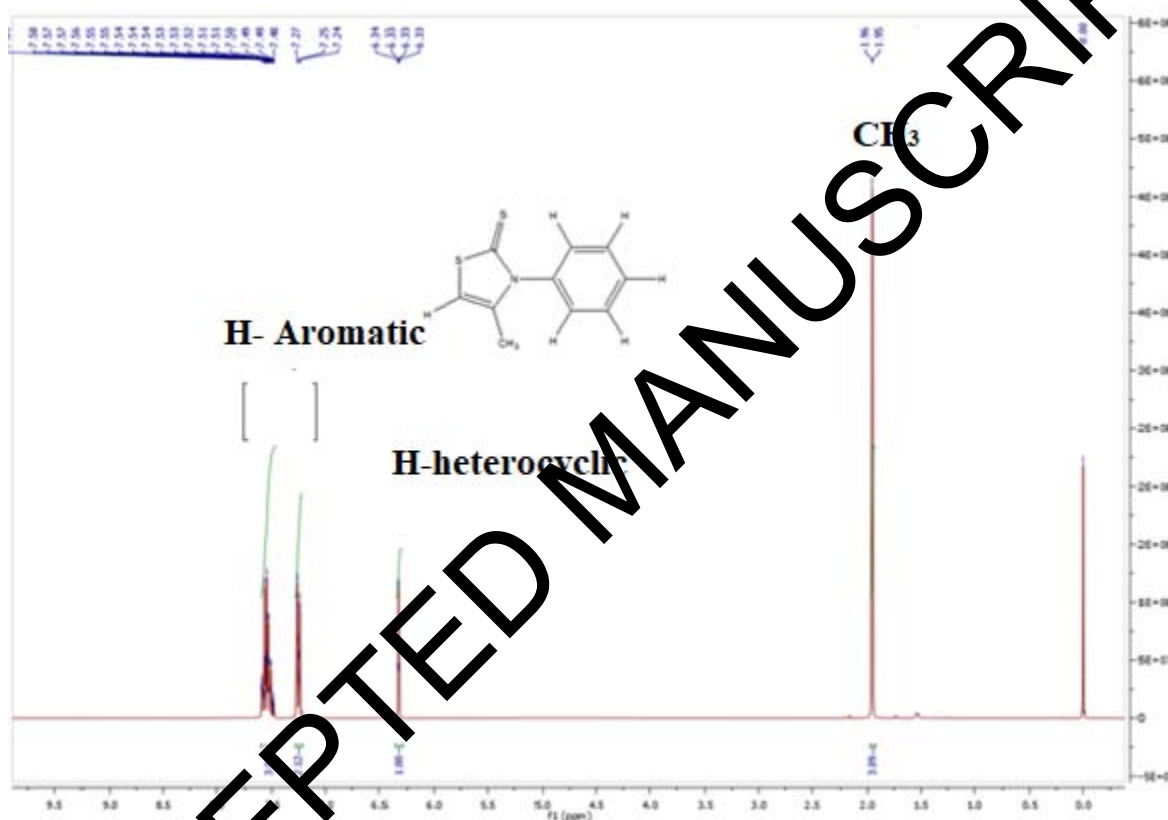


Figure 1b. NMR spectra of 4-methyl-3-phenyl-2(3H)-thiazolethione (**TO1**)

b) 4-methyl-2-(methylthio)-3-phenylthiazol-3-ium (**ST1**)

The method adapted to the synthesis of this thiazolium salt (**ST1**), provides the condensation of thiazolin-2-thione, with the alkyl iodine in acetonitrile with magnetic stirring at room temperature according to the alkylation method of thiazol-2-thione described by literature [20-21] as shown in figure 1c and NMR spectra of **ST1** is presented in figure 1d.

In a 200 ml monocolumn flask, 100 mg (10 mmol, 2 g, 1 eq) of thiazolin-2-thione are solubilized in acetonitrile (50 ml). Then 6.84 ml (11 eq) of methyl iodide is added using a syringe. The solution is stirred magnetically for 24 h at room temperature. The product is obtained by sinter filtration and dried (85%, mp = 220°C).

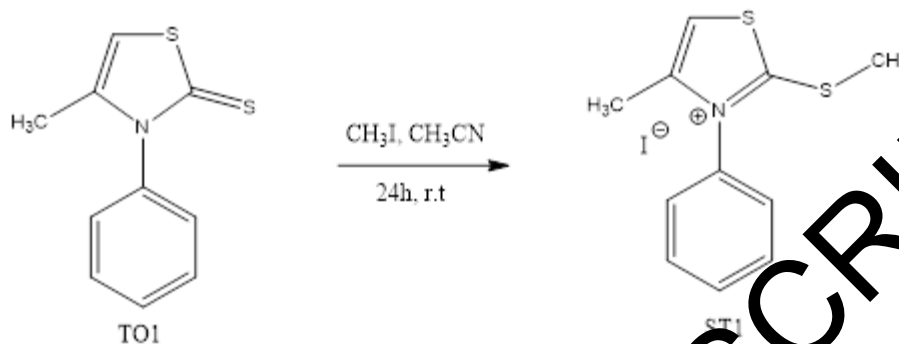


Figure 1c. Synthesis thiazolium iodides via thiazolin-2-thione.

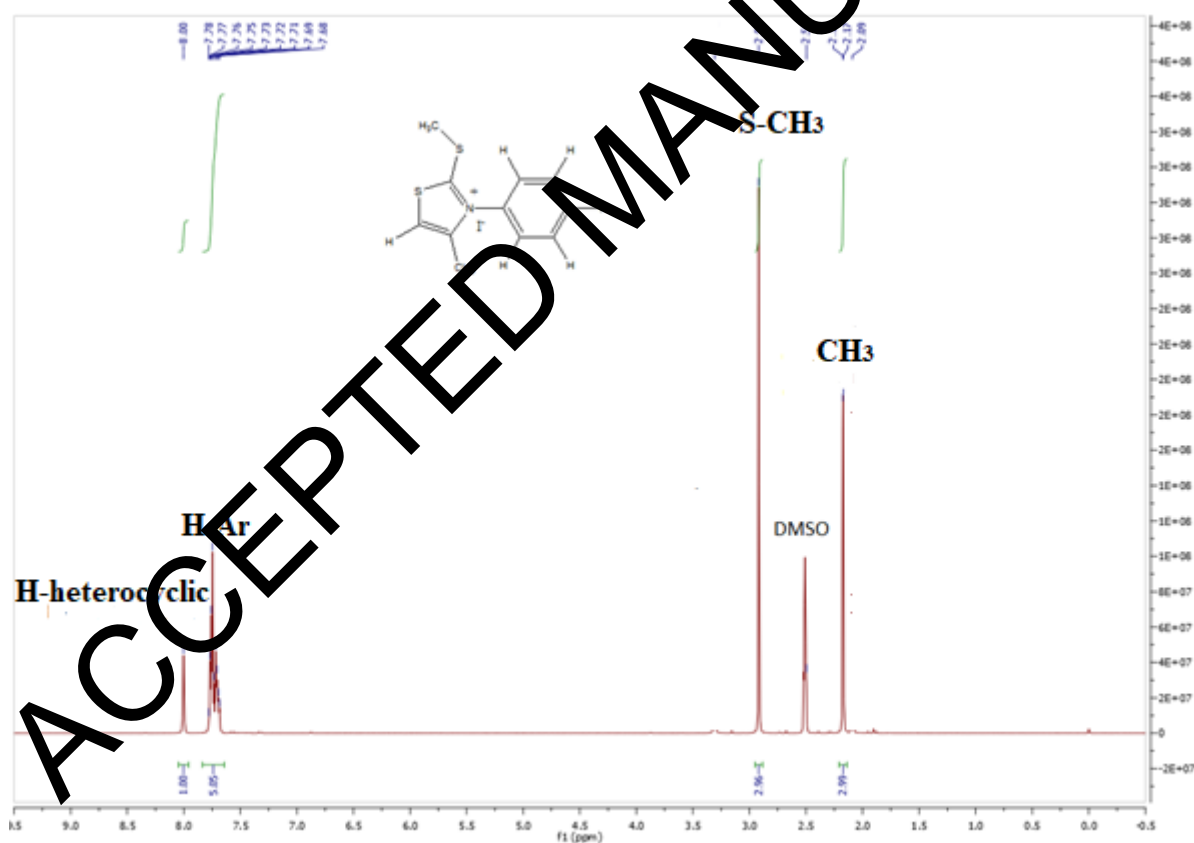


Figure 1d. NMR spectra of 4-methyl-2-(methylthio)-3- phenylthiazol-3-ium (ST1)

2.2. Methods

For weight loss studies the dimension of C38 steel is 1.5 cm × 1.5 cm × 0.2 cm. The measurements were carried out at 30°C for 1 h of immersion into 100 mL of 1 M hydrochloric acid in the absence and the presence of various concentrations of inhibitors.

After immersion, the samples were washed, degreased with acetone and weighed. All the manipulations were repeated three times in order to have reproducibility. Equations (1), (2) and (3) give the procedure for calculating the corrosion rate (C.R), the inhibitory efficiency (IE%) and the recovery rate () [4]:

$$\text{C.R} = \frac{\Delta W}{S \times t} \quad (1)$$

where ΔW = weight loss (mg), S = area of specimen (cm^2), and t = exposure time (hours).

$$\text{IE\%} = \frac{\text{C.R} - \text{C.R}'}{\text{C.R}} \times 100 \quad (2)$$

$$\text{Recovery rate} = \frac{\text{C.R} - \text{C.R}'}{\text{C.R}'} \times 100 \quad (3)$$

where C.R and C.R' are the corrosion rate with and without inhibitor, respectively.

Electrochemical measurements were carried out at a temperature of 30 °C in a Pyrex glass thermostatted cell with three electrodes (carbon steel C38 as working electrode with an area of 1 cm^2 , platinum as counter-electrode (1 cm^2) and a saturated calomel electrode as reference electrode). The solution is subjected to stirring and azote gas bubbling. The Solartron Instruments SI 1287 potentiostat assisted by a personal computer via a GPIB interface and the CorrWare 2.80 software were used to perform the electrochemical tests and collect the experimental data. The steel sample was allowed to corrode freely and its open circuit potential (OCP) for 1 hour (sufficient time to have the stable potential regime). The last OCP value recorded corresponds to the corrosion potential (E_{corr}) of the working electrode.

The inhibition efficiency (IE %) was calculated using the following equation:

where i_0 and i_{inh} are corrosion current without and with inhibitor, respectively.

AC impedance measurements were performed with the same electrochemical system using ZPlot 2.80 and ZView 2.80 software to fit the spectra obtained. The system was excited with alternating current with frequency range from 10^5 Hz to 10^{-2} Hz and a peak-to-peak amplitude of 10 mV with 10 points per decade. All EIS diagrams were registered at E_{corr} potential. The values of charge transfer resistance were used to calculate the inhibition efficiency (IE_{Rt} (%)) as previously described [4].

The detailed description of the method X-ray photoelectron spectroscopy (XPS) as well as the treatment of the results is given in our published paper [4].

3. Results and Discussion

3.1. Weight loss measurements

The table 1 gives the values of the corrosion rate and inhibition efficiency of **TO1** and **ST1** in 1M HCl. An overview on this table, we clearly notice that the both inhibitors are effective against corrosion, even at low concentration and that their efficacies are related to the inhibitor concentrations.

Maximum IE% of each compound was achieved at $2 \cdot 10^{-4}$ M for **TO1** and 10^{-3} M for **ST1**. The use of lower concentration for the **TO1** inhibitor can be explained in terms of non-binding pairs in the molecule. While **TO1** has two unbonded electron pairs, the **ST1** molecule has only one pair. This fact indicates a greater adsorption and attraction to the metal of the **TO1** inhibitor.

Table 1. Weight loss results of C38 carbon steel in presence of **TO1** and **ST1** in 1M HCl

Conc.	Corrosion rate	IE
(M)	(mg.cm ² .h ⁻¹)	(%)

	Blank	1.00	----
TO1	10^{-6}	0.61	39
	10^{-5}	0.42	58
	10^{-4}	0.22	78
	2.10^{-4}	0.07	93
ST1	10^{-6}	0.48	52
	10^{-5}	0.30	70
	10^{-4}	0.24	76
	5.10^{-4}	0.13	87
	10^{-3}	0.06	94

Moreover, we note from the same table that the **ST1** is more efficient compared to the **TO1** at the concentration lower than 10^{-4} M. This is probably due to the strong adsorption at low concentration of the compound **TO1** compared to **ST1**.

3.2. Electrochemical experiment

3.2.1. Polarization curves

Under the same conditions as the gravimetric measurements ($t = 1$ h and $T = 30^{\circ} \text{C}$), the anodic and cathodic polarization curves in the absence and in the presence of both inhibitors at different concentrations were obtained (figure 2a and 2b). The scan rate of the electrochemical tests is 0.5 mV/s [22-23].

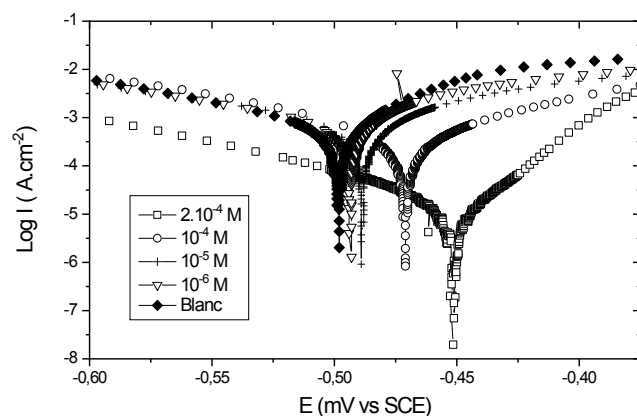


Figure 2a. Potentiodynamic polarization curves for C38 steel in 1 M HCl containing different concentrations of TO1.

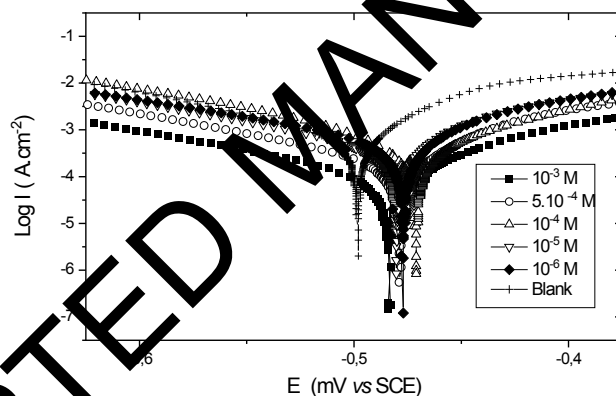


Figure 2b. Potentiodynamic polarization curves for C38 steel in 1 M HCl containing different concentrations of S11.

In both inhibitors, a decrease in the anodic and cathodic currents is observed. The values extracted from these figures such as corrosion potential, Tafel slopes, corrosion current and inhibitor efficiency are shown in table 2.

From this table, we can draw the following conclusions:

- The presence of the two inhibitors moves the E_{corr} values towards anodic values.

- As reported elsewhere, when the values of corrosion potential in the presence of inhibitor is greater than ± 85 mV compared to the value in the absence of inhibitor, the inhibitor is considered to be either anodic or cathodic. In this study, the maximum displacement in corrosion potential observed is ± 32 mV suggests that the two inhibitors behaves as mixed type of inhibitor [4].
- The values of b_c change with increasing concentration of both inhibitors. These results indicate that the kinetic of the hydrogen evolution reaction is influenced by the presence of **TO1** and **ST1**. Such behavior has been largely observed and discussed in the literature [24-25].
- The increase in the concentration of inhibitors has the consequence of increasing their inhibition efficiency.

Table 2. Electrochemical potentiodynamic polarization parameters for C38 steel in 1 M HCl containing **TO1** and **ST1**.

	Conc. (Mol/L)	$-E_{\text{corr}}$ (mV/s SCE)	$-b_c$ (mV/dec)	I_{corr} (mA / cm ²)	EI_{corr} (%)
	E_{anc}	-498	138	1115	----
TO1	10^{-6}	-494	137	796	28.60
	10^{-5}	-488	106	500	55.15
	10^{-4}	-470	52	253	77.30
	2.10^{-4}	-466	73	34	96.95
ST1	10^{-6}	-477	135	529	52.55
	10^{-5}	-491	96	348	68.78
	10^{-4}	-473	65	305	72.64
	5.10^{-4}	-486	85	160	85.65
	10^{-3}	-487	93	70	93.72

3.2.2. The electrochemical impedance spectroscopy (EIS)

Nyquist Impedance diagrams obtained at E_{corr} for C38 steel in HCl 1M in the absence and in the presence of **TO1** and **ST1** are given in figure 3 (a and b).

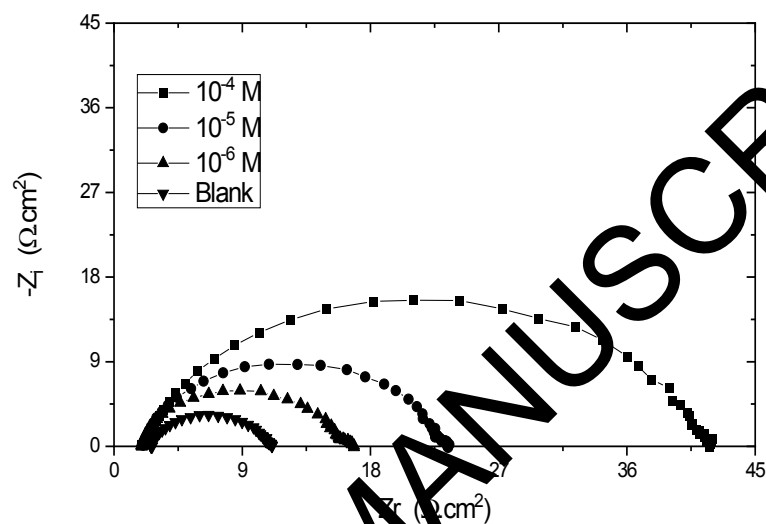


Figure 3a. Nyquist plot for C38 steel in 1 M HCl with and without **TO1** at 30°C.

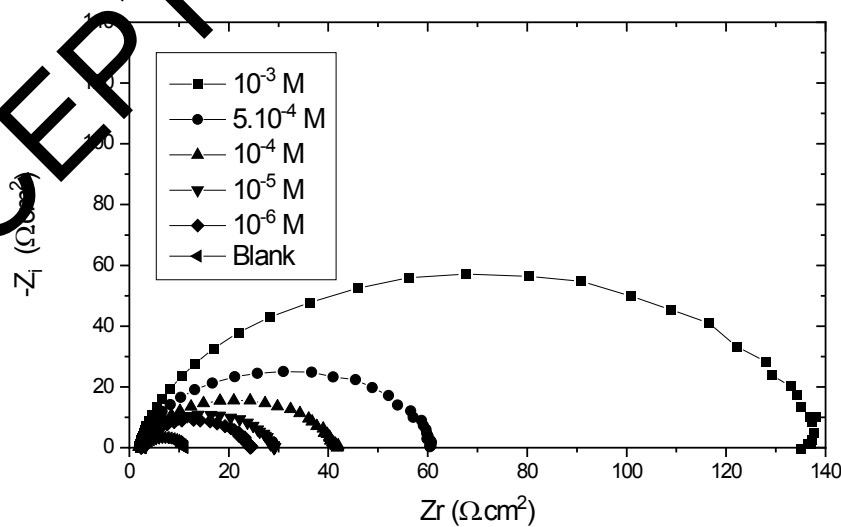


Figure 3b. Nyquist plot for C38 steel in 1 M HCl solution with and without **ST1** at 30°C.

The diagrams are not perfect semicircles and have been attributed to frequency dispersion [26]. This approximately semicircular of impedance diagrams shows that the corrosion phenomenon is controlled by a charge transfer process [6, 27-29]. The increasing of the diameter with increasing of the concentration of the inhibitor indicates the good inhibition effect of our inhibitor [6]. The modeling of these diagrams by the ZView software led us to propose the following equivalent electrical circuit: an electrolyte resistor in series with a charge transfer resistor which in parallel with a CPE (figure 4).

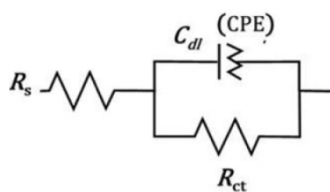


Figure 4. Electrical equivalent circuit

The obtained results are given in Table 3 (the charge transfer resistance R_t , n values, the CPE (Q) values, the double layer capacitance C_{dl} and inhibition efficiency). Detailed method of calculating C_{dl} values from CPE values is identical to that given in our previous work [4].

It can be seen that the presence of the two inhibitors affects the values of R_t towards the high values and the values of C_{dl} in the opposite direction. On the otherhand, in all the case of TO1 and ST1, n reaches approximately the same value of 0.80. This result can be interpreted as an indication of the degree of heterogeneity of the metal surface, corresponding to a small depression of the double layer capacitance semicircle.

These results confirmed the obtained results by the above methods.

Table 3. Impedance parameters for the corrosion of the system C38 steel / 1 M HCl in the presence of TO1 and ST1.

Conc.	R_t	Q	n	C_{dl}	EI_{Rt}
(Mol/L)	($\Omega \cdot \text{cm}^2$)	($\Omega^{-1} \cdot \text{cm}^{-2} \cdot \text{s}^n$)		($\mu\text{F cm}^{-2}$)	(%)

	Blank	7.77	9.81×10^{-4}	0.8	290	----
	10^{-6}	13.57	7.05×10^{-4}	0.79	205	42.74
	10^{-5}	20.02	4.84×10^{-4}	0.78	131	61.18
TO1	10^{-4}	36.4	3.24×10^{-4}	0.80	107	78.65
	2.10^{-4}	252.8	6.7×10^{-5}	0.79	23	98.80
	10^{-6}	20.69	5.14×10^{-4}	0.81	177	62.44
	10^{-5}	25.08	4.30×10^{-4}	0.78	120	69.01
ST1	10^{-4}	36.4	3.24×10^{-4}	0.80	107	78.65
	5.10^{-4}	55.55	2.35×10^{-4}	0.82	91	86.01
	10^{-3}	126.7	1.08×10^{-4}	0.80	37	93.86

3.3. Adsorption isotherm

The Langmuir adsorption isotherm is plotted in the figure 4 (example for **ST1**) using the parameters from weight loss measurements and the following equation ($C_{inh}/\theta = 1/K + C_{inh}$) with C_{inh} is the inhibitor concentration, the θ is the degree of surface coverage and K is the adsorption constant [30-31].

The plot of C/θ vs. C (Fig. 5) yields a straight line with correlation coefficient close to 1. The Values of K was found to be $1.42 \times 10^5 \text{ M}^{-1}$ and $0.71 \times 10^5 \text{ M}^{-1}$ for **TO1** and **ST1** respectively. The strong adsorption of the two inhibitors on C38 steel surface is reflected by high value of adsorption equilibrium constant.

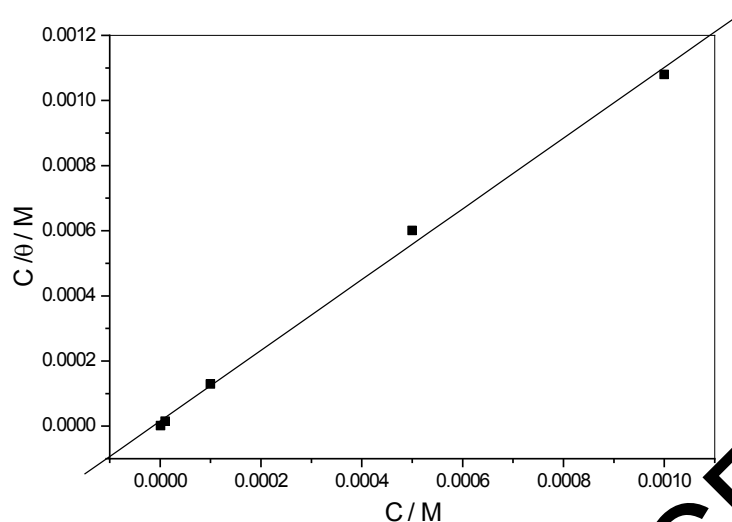


Figure 5. Curve fitting of the corrosion data of C38 steel in the presence of **ST1** to Langmuir isotherm

The relation between the standard free enthalpy, ΔG_{ads} , and the adsorption constant (K) is given by the relation:

$$K = 55.5 \exp(-\Delta G_{\text{ads}}/RT)$$

The ΔG_{ads} was calculated as -40.0 kJ/mol and -38.05 kJ/mol for **ST1** and **TO1** respectively.

The spontaneous adsorption of the two molecules on the metal surface is clearly identified by the large negative values of the standard absorption enthalpy.

According to the literature, values of ΔG_{ads} around of -40 KJ.mol⁻¹ or less are attributed to the formation of strong covalent bonds between the surface of the metal and the free electrons existing on the heteroatoms of the inhibitory molecules therefore chemisorption [27, 32-34]. In our study, the calculated values of ΔG_{ads} indicate the chemisorptive nature of the adsorption of inhibitors in 1M HCl solution [35-36].

The use of thiazole derivatives as corrosion inhibitors has been discussed in several publications [37-42]. Table 4 shows the protection efficiency and ΔG_{ads} obtained of some thiazole derivatives exploited as corrosion inhibitors of steel in a 1 M HCl medium. Such comparison shows that the values of the standard free enthalpy (ΔG_{ads}) obtained in our study

and those of the literature are in good agreement where we clearly notice that the majority of thiazole derivatives are strongly adsorbed with a mixed adsorption (physisorption with a tendency to chemisorption).

Table 4. Corrosion protection parameter for thiazole derivatives in 1M HCl

Thiazole derivative	Optimum Concentration	Metal	Protection efficiency	$-\Delta G_{ads}$ (kJ/mol)
4-methyl-3-phenyl-2(3H)-thiazolethione [this work]	2×10^{-4} M	C38 steel	98.80%	40.0
thiazol: 4-methyl-2-(methylthio)-3-phenylthiazol-3-ium [this work]	10^{-3} M	C38 steel	93.86%	38.05
3-((4-amino-2-methylpyrimidin-5-yl)methyl)-5-(2-hydroxyethyl)-4-methylthiazol-3-ium chloride [37]	40 ppm	Carbon steel	91.3%	48
4-(pyridin-4-yl)thiazol-2-amine [38]	2×10^{-4} M	Mild steel	96.06%	36.33
2-(2'-hydroxyphenyl)benzothiazole [39]	50 ppm	Mild steel	92.1%	34.31
2-(2',5'-dihydroxyphenyl)benzothiazole [39]	50 ppm	Mild steel	51.6%	31.87
(4-benzothiazole-2-yl-phenyl)-dimethyl-amine [39]	50 ppm	Mild steel	96.8%	40.80
2-(n-hexylamino)-4-(3 -N,N-dimethylamino-propyl)amino-6-(benzothiazol-2-yl)thio-1,3,5-s-triazine [40]	10^{-3} M	Carbon steel	99%	34.09
and 2-(n-octylamino)-4-(3 -N,N-dimethylaminopropyl)amino-6-(benzothiazol-2-yl)thio-1,3,5-s-triazine [40]	10^{-3} M	Carbon steel	99.3%	37.92
Mercaptobenzothiazole [40]	10^{-3} M	Carbon steel	57.3%	31.72
4-(1-hexadecyl-1H-benzo[d]imidazol-2-yl)thiazole [41]	10^{-3} M	Mild steel	94.5%	38.2
1,3-bis(hexadecyl-2-(thiazol-4-yl)-1H-benzo[d]imidazol-3-ium)bromide [41]	10^{-3} M	Mild steel	95.3%	41.6
2-(2-Hydroxyphenyl)benzothiazole [42]	7.10^{-5} M	Mild steel	96.8%	-37

3.4 Analysis of the organic film formed by XPS photoelectron spectroscopy

For a better understanding of the inhibition mechanism, we performed photoelectron spectroscopy (XPS) surface analyzes on the organic inhibitor alone and on the organic film adsorbed on the steel surface. In this case we study only the results of **TO1** compound.

The characterization by XPS is carried out on the pure **TO1** pressed in the form of a pellet (13x2x2 mm³) and on the steel disc immersed for 24 hours in 1M HCl in the presence of the optimal concentration of **TO1** (2×10^{-4} M). The latter is removed from the corrosive medium, rinsed with distilled water and degreased in ethanol under ultrasound and finally dried. The presence of TO1 on the steel surface was detected based on the signal characteristic of the sulfur atom S2p (Fig. 6b). For comparative purposes, the XPS spectrum of pure TO1 (Fig. 6a) were also obtained.

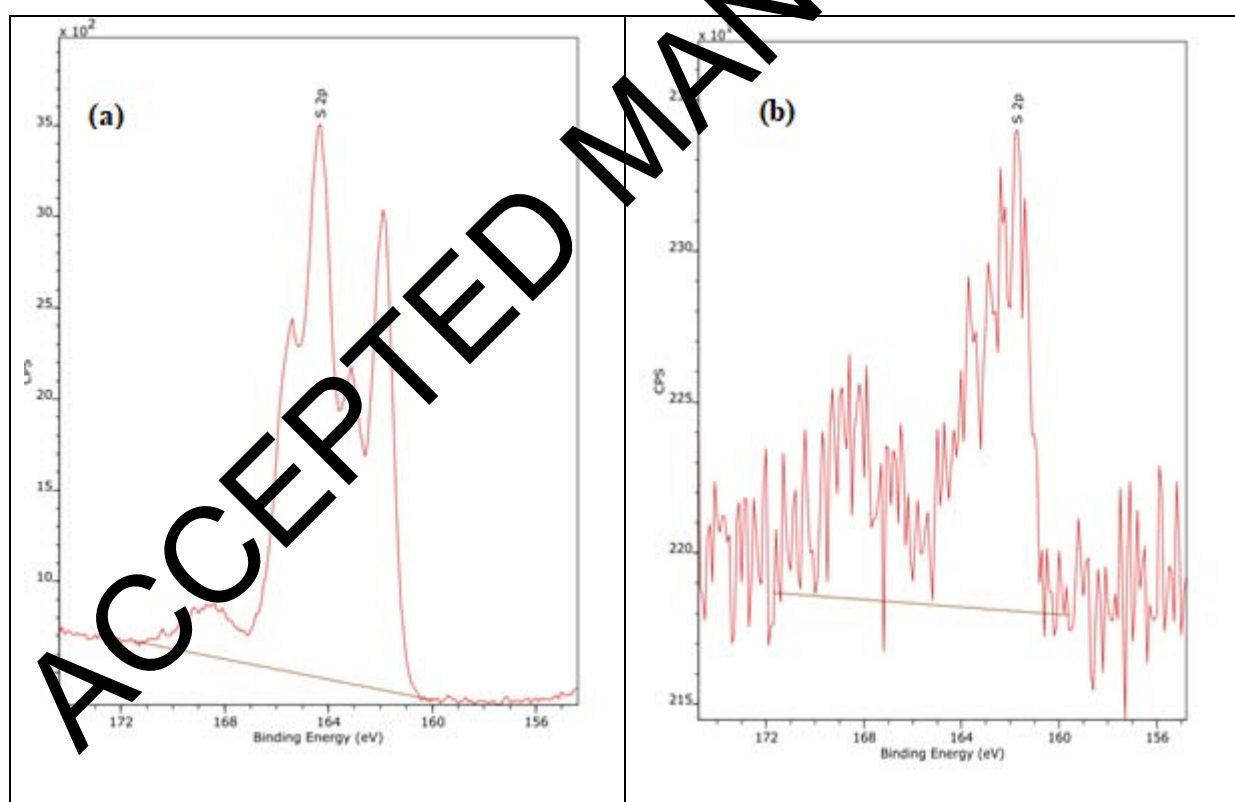


Figure 6. XPS spectrum of S2p for: (a) pure TO1 and (b) the surface of the steel exposed to the solution (2×10^{-4} M **TO1** + 1M HCl) for 24 h at 30 ° C.

For the surface exposed to hydrochloric acid containing TO1, the large signal from sulfur observed in the binding energy range of 161 to 172 eV, can be attributed to several

components with different binding energies. We observed that the S2p peaks can be deconvoluted into several components formed of three doublets. The first deconvoluted peak in 162.0 and 163.3 eV is attributed to the oxidation states of sulfur. The doublet at 164.6 and 165.9 eV, which is characteristic of the thione function and thiazole (structure --S--), shows the presence of **TO1** on the steel surface [43] and a doublet at 168.5 and 169.8 eV is due to the presence of sulphates, SO_4^{2-} which is due to the oxidation of S^{2-} [44-45].

The surface of the steel covered by chemisorbed **TO1** molecules (Fig. 7) reveals the existence of a binding energy component to 711 eV ($\text{Fe}2p_{3/2}$) and at 724 eV ($\text{Fe}2p_{1/2}$) characteristic of Fe^{3+} , showing the oxidation of the steel surface [46-47]. The same figure shows a little $\text{Fe}2p$ peak at 706.6 eV characteristic of Fe^0 [48-49]. The increase in the $\text{Fe}2p$ signal confirms the adsorption and the film formation on the steel surface [50-51].

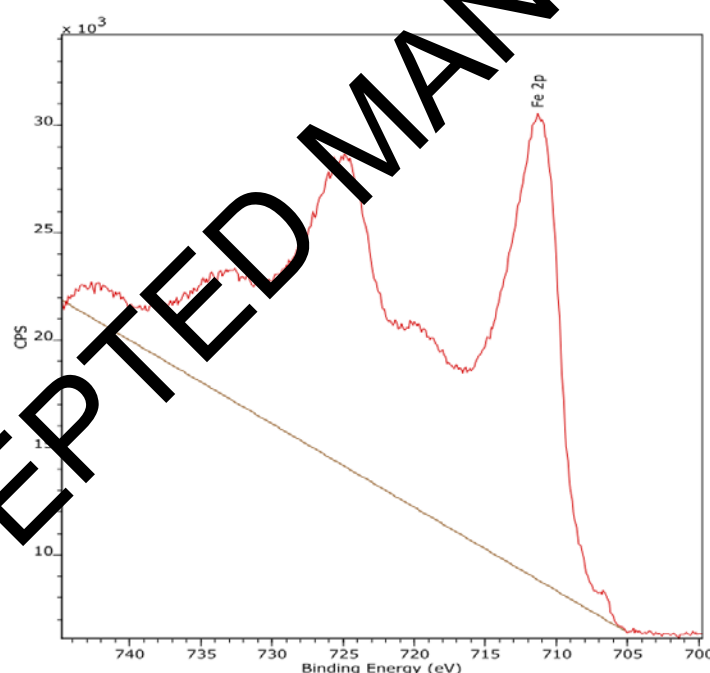


Fig. 7. Spectre $\text{Fe}2p$ pour la surface de l'acier oxydée exposée à une solution (2×10^{-4} M **TO1** + HCl 1M) pendant 24 h à 30°C .

N 1s spectrum of metal treated with **TO1** in 1 M HCl shows one peak located at around 399 - 402 eV (Fig. 8). This peak can be partly associated to $=\text{N--}$ structure in the thiazole ring [52].

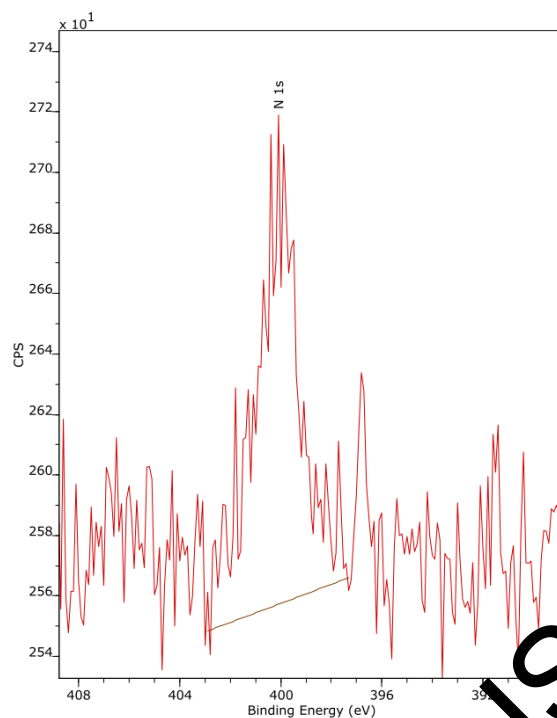


Fig. 8. XPS profile of N 1s for TO1-treated steel.

3.4. Conclusion

The results of inhibition of two compounds (**TO1** and **ST1**) were studied in 1 M HCl for corrosion of C38 steel by different methods (weight loss and the electrochemical measurements). **TO1** and **ST1** appear as good inhibitors with better efficiency for **TO1**. The compounds under investigation were classified as cathodic type inhibitors. The above conclusions were confirmed by EIS study where the charge transfer resistance increases and double layer capacitance decreases as the concentration of the inhibitor increases. Adsorption of **TO1** and **ST1** on the C38 steel surface obeyed to the Langmuir isotherm. An XPS spectrum confirms that the adsorption of the two molecules was done through nitrogen and sulfur atoms.

References

1. F. Fadel, D. Ben Hmamou, R. Salghi, B. Chebli, O. Benali, A. Zarrouk, E. E. Ebenso, A. Chakir, B. Hammouti, Antifungal activity and anti-corrosion inhibition of

- origanum compactum extracts, Inter. J. Electrochem. Sci., 82013 (2013) 11019-11032.
2. H. B. Ouici, M. Tourabi, O. Benali, C. Selles, M. Traisnel, C. Jama, F. Bentiss, R. Salghil, Experimental investigation on the corrosion inhibition characteristics of mild steel by 5-(2-hydroxyphenyl)-1,3,4-oxadiazole-2-thiol in hydrochloric acid medium. Journal, Mater. Environm. Sci., 7(8) (2016) 2971-2988.
 3. H. B. Ouici, O. Benali, A. Guendouzi, Experimental and quantum chemical studies on the corrosion inhibition effect of synthesized pyrazole derivatives on mild steel in hydrochloric acid, Res. Chem. Intermed., 42 (9) (2016) 7085-7109.
 4. H. B. Ouici, M. Tourabi, O. Benali, C. Selles, C. Jama, A. Zerrouk, F. Bentiss, Adsorption and corrosion inhibition properties of 5-amino 1, 3, 4-thiadiazole-2-thiol on the mild steel in hydrochloric acid medium: Thermodynamic, surface and electrochemical studies, J. Electroanal. Chem., 803 (2017) 125-134.
 5. S. Gronowitz, in: S. Gronowitz (Ed.), The chemistry of heterocyclic compounds: thiophene and its derivatives, vol. 44, Wiley, (1991) New York, NY, USA, Part 3, (Chapter 2).
 6. K. D. Hargrave, F. K. Hess, J. T. Oliver, N-(4-Substituted-thiazolyl)oxamic acid derivatives, new series of potent, orally active antiallergy agents. J. Med. Chem., 26 (8) (1983) 1158-1163.
 7. I. Hutchinson, S. A. Jennings, B. R. Vishnuvajjala, A. D. Westwell, M. F. G. Stevens, Antitumor Benzothiazoles. 16.1 Synthesis and Pharmaceutical Properties of Antitumor 2-(4-Aminophenyl)benzothiazole Amino Acid Prodrugs, J. Med. Chem., 45 (3) (2002) 744-747.
 8. D. J. Kempf, H. L. Sham, K. C. Marsh, C. A. Flentge, D. Betebenner, B. E. Green, E. McDonald, S. Vasavanonda, A. Saldivar, N. E. Wideburg, W. M. Kati, L. Ruiz, C.

- Zhao, L. Fino, J. Patterson, A. Molla, J. J. Plattner, D. W. Norbeck, Discovery of ritonavir, a potent inhibitor of HIV protease with high oral bioavailability and clinical efficacy, *J. Med. Chem.*, 41 (4) (1998) 602-617.
9. M. V. Nora de Souza, Synthesis and biological activity of natural thiazoles: An important class of heterocyclic compounds. *J. Sulf. Chem.*, 26 (4-5) (2005) 429-449.
10. A. Rouf, C. Tanyeli, Bioactive thiazole and benzothiazole derivatives. *Euron. J. Med. Chem.*, 97 (5) (2015) 911-927.
11. W. C. Patt, H. W. Hamilton, M. D. Taylor, M. J. Ryan, D. G. J. Taylor, Structure-activity relationships of a series of 2-amino-4-thiazole-containing renin inhibitors, *J. Med. Chem.*, 35 (14) (1992) 2562-2572.
12. R. N. Sharma, F. P. Xavier, K. K. Vasu, S. C. Chaturvedi, S. S. Pancholi, Synthesis of 4-benzyl-1,3-thiazole derivatives as potential anti-inflammatory agents: an analogue-based drug design approach, *J. Enzyme Inhib. Med. Chem.*, 24 (3) (2009): 890-897.
13. A. A. Al-Sarawy, A. S. Fouda, W. A. S. El-Dein, Some thiazole derivatives as corrosion inhibitors for carbon steel in acidic medium, *Desalination*, 229 (2008) 279–293.
14. M. Zebida, O. Benali, U. Maschke, M. Trainsel, Corrosion inhibition properties of 4-methyl-2-(methylthio)-3-phenylthiazol-3-ium iodide on the carbon steel in sulfuric acid medium, *Inter. J. Corros. Scale Inhib.*, 8(3) (2019) 613–627.
15. F. Y. Cui, L. Guo, S.T. Zhang, Experimental and theoretical studies of 2-aminothiazole as an inhibitor for carbon steel corrosion in hydrochloric acid, *Mater. Corros.*, 65 (2014) 1194–1201.
16. A. Döner, R. Solmaz, M. Özcan, G. Kardaş, Experimental and theoretical studies of thiazoles as corrosion inhibitors for mild steel in sulphuric acid solution, *Corros. Sci.*, 53 (9) (2011) 2902–2913.

17. T. Eicher, S. Hauptmann, A. Speicher, The chemistry of heterocycles: structure, reactions synthesis and applications, 2nd Edition (2003) Wiley-VCH, Weinheim.
18. L. Guo, X. Ren, Y. Zhou, S. Xu, Y. Gong, S. Zhang, Theoretical evaluation of the corrosion inhibition performance of 1,3-thiazole and its amino derivatives, Arab. J. Chem., 10 (2017) 121-130.
19. C. Roussel, M. Adjimi, A. Chemlal, A. Djafri, Comparison of racemization processes in 1-arylpyrimidine-2-thione and 3-arylthiazoline-2-thione atropisomers and their oxygen analogs, J. Org. Chem., 53 (1988) 5076-5080.
20. C. Roussel, F. Andreoli, M. Roman, M. Hristova, N. Vantuyne, New route to 3-alkylthiazolo[3,2-a]benzimidazole derivatives, Molecules, 10 (2005) 327–333.
21. O. Benali, L. Larabi, B. Tabti, Y. Harek, Influence of 1-methyl 2-mercapto imidazole on corrosion inhibition of carbon steel in 0.5 M H₂SO₄, Anti-corros. Meth. Mater., 52 (5) (2005) 280-285.
22. F. Bentiss, M. Traisnel, M. Lagrenée, The substituted 1,3,4-oxadiazoles: a new class of corrosion inhibitors of mild steel in acidic media, Corros. Sci., 42 (1) (2000) 127-146.
23. F. Mansfeld, M. V. Kending, S. Tsai, Recording and analysis of AC impedance data for corrosion studies. Corrosion, 38 (11) (1982) 570-580.
24. L. Larabi, O. Benali, Y. Harek, Corrosion inhibition of cold rolled steel in 1 M HClO₄ solutions by N-naphtyl N'-phenylthiourea. Mater. Lett., 61 (2007) 3287–3291.
25. M. B. Ouici, O. Benali, Y. Harek, L. Larabi, B. Hammouti, A. Guendouzi, Inhibition of mild steel corrosion in 5 % HCl solution by 5-(2-hydroxyphenyl)-1,2,4-triazole-3-thione. Res. Chem. Intermed., 39 (2013) 2777–2793.

26. O. Benali, L. Larabi, S. M. Mekelleche, Y. Harek, Influence of substitution of phenyl group by naphthyl in a diphenylthiourea molecule on corrosion inhibition of cold-rolled steel in 0.5 M H₂SO₄, *J. Mater. Sci.*, 41 (2006) 7064–7073.
27. O. Benali, A. Benikdes, D. Ben Hmamou, Adsorption and Corrosion Inhibitive Properties of 1-Methyl-1H-imidazole-2- thiol on Mild Steel in Acidic Environment, *Pharm. Chem. J.*, 7(3) (2020) 56-68.
28. O. Benali, M. Zebida, U. Maschke, A. Attou, S. Bilgiç, Synthesis of 4-methylthiazol-2(3H)-thione derivatives and their application as corrosion inhibitors. Weight loss, electrochemical, XPS and theoretical study, *Appl. J. Envir. Eng. Sci.*, 7(2) (2021) 125-143.
29. H. B. Ouici, O. Benali, Y. Harek, L. Larabi, B. Hammoudi, A. Guendouzi, The effect of some triazole derivatives as inhibitors for the corrosion of mild steel in 5 % hydrochloric acid, *Res. Chem. Intermed.* 39 (2013) 3089–3103.
30. A. Attou, A. Benikdes, O. Benali, H.B. Ouici, A. Guendouzi, Experimental studies on the corrosion inhibition effect of new synthesized pyrazole derivatives on C38 steel in 0.5 M H₂SO₄ and HCl 1M, *Inter. J. Chem. Biochem. Sci.*, 17 (2020) 120-128
31. F. Chaib ,H. Alali, O. Benali, Guido Flamini, Corrosion inhibition effects of the essential oils of two Asteraceae plants from South Algeria, *Inter. J. Chem. Biochem. Sci.* 18(2020):129-136.
32. M. Jeeva, G. V. Prabhu, M. S. Boobalan, C. M. Rajesh,. Interactions and inhibition effect of urea-derived mannich bases on a mild steel surface in HCl. *J. Phys. Chem., C*, 119 (38) (2005) 22025–22043.
33. Z. Szklarska-Smialowska, J. Mankowski, Crevice corrosion of stainless steels in sodium chloride solution, *Corros. Sci.*, 18 (11) (1978) 953 - 960.

- 34 A. Yurt, S. Ulutas, H. Dat, Electrochemical and theoretical investigation on the corrosion of aluminium in acidic solution containing some Schiff bases, *Appl. Surf. Sci.*, 253 (2) (2006) 919-925.
- 35 M. Hegde, S. P. Nayak, Synthesis, Characterization and study of new thiazole -2-amine derivative as corrosion inhibitors for mild steel in 0.5 M H₂SO₄ solution. *J. Chem. Pharm. Sci.*, 1 (2018)16-24.
- 36 C. J. Zou, X. L. Yan, Y. B. Qin, M. Wang, Y. Liu, Inhibiting evaluation of β -Cyclodextrin-modified acrylamide polymer on alloy steel in sulfuric solution, *Corros. Sci.*, 85 (2014) 445–454.
- 37 A. A. Farag, M. A. Migahed, E. A. Badr, Thiazole Ionic Liquid as Corrosion Inhibitor of Steel in 1 M HCl Solution: Gravimetical, Electrochemical, and Theoretical Studies. *Journal of Bio- and Tribo-Corrosion* (2019) 5:53. <https://doi.org/10.1007/s40735-019-0246-4>
- 38 X Yang, F. Li, W. Zhang, 4-(Pyridin-4-yl)thiazol-2-amine as an efficient nontoxic inhibitor for mild steel in hydrochloric acid solutions, *RSC Adv.*, 2019, 9, 10454-10464.
- 39 Z. Salarvand, M. Amirnasr, M. Talebian, K. Raeissi, S. Meghdadi, Enhanced corrosion resistance of mild steel in 1 M HCl solution by trace amount of 2-phenyl-benzothiazole derivatives: Experimental, quantum chemical calculations and molecular dynamics (MD) simulation studies, *corrosion science* 114 (2017) 133-145.
- 40 Z. Hu, Y. Meng, X. Ma, H. Zhu, J. Li, C. Li, D. Cao, Experimental and theoretical studies of benzothiazole derivatives as corrosion inhibitors for carbon steel in 1 M HCl, *Corrosion Science*, 112 (2016) 563-575.

- 41 N. Abdulwali1, F. Mohammed, A. Al subari, H. Ghaddar, A. Guenbour, A. Bellaouchou, E. Essassi, R. A. Cottis, Effect of Thiazole Derivatives on the Corrosion of Mild Steel in 1 M HCl Solution, *Int. J. Electrochem. Sci.*, 9 (2014) 6402 – 6415
- 42 S. Xu, W. Li, X. Zuo, D. Zheng, X. Zheng, S. Zhang, Structural Origin of Corrosion Inhibition Effect over 2-(2- Hydroxyphenyl)benzothiazole on Steel in HCl Medium, *Int. J. Electrochem. Sci.*, 14 (2019) 5777 – 5793, doi: 10.20964/2019.06.20.
- 43 R. Riga et J.J. Verbist, *J. Chem. Soc. Perkin Trans., II*, 1545 (1983).
- 44 A. Olsson, P. Agrawal, M. Frey et D. Landolt, *Corros. Sci.*, 42, 1211 (2000).
- 45 M. Labrini, Synthèses et études physicochimiques de nouveaux thiadiazoles inhibiteurs de corrosion de l'acier en milieu acide, Thèse de doctorat, Université de des sciences et de technologie de Lille, 2005, France.
- 46 R. Devaux, D. Vouagner, A.M. De Becdelieuvre et C. Duret-Thual, *Corros. Sci.*, 36, 171 (1994).
- 47 V. Di castro et S. Ciampi, *Surf. Sci.*, 331, 294 (1995).
- 48 T.L. Barr, *J. Phys. Chem.*, 82, 1801 (1978).
- 49 A.S. Lima et A. Attens, *Appl. Phys.*, 51, 411 (1990).
- 50 A. P. Grosvenor, B. A. Kobe, M. C. Biesinger, N. S. McIntyre, Investigation of multiple splitting of Fe 2p XPS spectra and bonding in iron compounds, *Surf. Interf. Anal.*, 36 (2004) 1564-1574.
- 51 J. C. Dupin, D. Gonbeau, P. Vinatier, A. Levasseur, Systematic XPS studies of metal oxides, hydroxides and peroxides, *Phys. Chem. Chem. Phys.*, 2 (2000) 1319-1324.
- 52 F. Moulder, W.F. Stickle, P.E. Sobol, K.D. Bomben, in: J. Chastain (Ed.), *Handbook of X-Ray Photoelectron Spectroscopy*, Perkin-Elmer Corp., Minnesota, USA, 1995.

ACCEPTED MANUSCRIPT